ELSEVIER

Carbohydrate Research 337 (2002) 1633–1640

CARBOHYDRATE RESEARCH

www.elsevier.com/locate/carres

Conformation of the branched O-specific polysaccharide of *Shigella dysenteriae* type 2: Molecular mechanics calculations show a compact helical structure exposing an epitope which potentially mimics galabiose

Jimmy Rosen, Armin Robobi, Per-Georg Nyholm*

Department of Medical Biochemistry, Centre for Structural Biology, Göteborg University, Medicinaregatan 7B, SE-405 30 Göteborg, Sweden

Received 30 September 2001; received in revised form 18 March 2002; accepted 25 March 2002

Abstract

Conformational analyses of the branched repeating unit of the O-antigenic polysaccharide of *Shigella dysenteriae* type 2 have been performed with molecular mechanics MM3. A filtered systematic search on the trisaccharide α-D-GalNAc-(1→3)-[α-D-Glc-NAc-(1→4)]-α-D-GalNAc forming the branch, shows essentially a single favored conformation. Also, the downstream α-D-Gal-NAc-(1→4)-α-D-Glc linkage is sterically constrained. The α-D-Glc-(1→4)-β-D-Gal moiety, however, forms a more flexible link region between the branch points, and shows a 90° bend similar to what is known for the galabiose moiety occurring in globo-glycolipids. The calculations indicate that consecutive repeating units in their minimum energy conformation arrange in a helical structure with three repeating units per turn. This helix is very compact and appears to be stabilized by hydrophobic interactions involving the N-acetyl groups at the branch points. Random conformational search suggests the existence of another helical structure with four repeating units per turn. It appears possible that the α-D-Glc-(1→4)-β-D-Gal moiety, which is exposed on the surface of the helical structures, can evade recognition by the immune system of the host by the mimicry of globo structures.

Keywords: *Shigella dysenteriae*; O-Antigen; Conformation; Molecular mechanics; Molecular mimicry

1. Introduction

The *Shigella* bacteria, which give rise to serious enteric disease, shigellosis, with about 160 million new cases and 1.1 million deaths every year, are considered as important targets for vaccine development.[1] *Shigella dysenteriae*, which accounts for about 6% of all the cases of shigellosis, has been classified in ten different serotypes of which serotype 1 is considered to be the most severe pathogen.[1] The 3D structures of the O-specific polysaccharides of *Shigella* and other Gram negative bacteria are of great interest for a rational design of glycoconjugate vaccines.[2] The three-dimensional structure of the O-antigen of *S. dysenteriae* type 1 was recently reported based on NMR[3] and modeling[4] studies, and the antigenic properties of fragments of this polysaccharide have been studied in detail.[5,6] The serotypes of *S. dysenteriae* are not known to show cross-reactivity in reactions with antibodies, although most of these serotypes show certain structural similarities, in particular the presence of α-(1→3) links involving N-acetyl hexosamines.[7,8] The serotype 2, which gives rise to shigellosis in Guatemala, Hungary, and Yemen,[1] is of special interest conformationally since the O-antigen contains a branch point comprising three N-acetyl hexosamines, which are likely to give rise to steric constraints. The type 2 O-antigen has been synthesized,[9] but so far no conformational studies on this structure have been reported. We herein present the results of a molecular modeling study of the O-antigen of *S. dysenteriae* type 2, based on molecular mechanics (MM3) calculations.

* Corresponding author. Fax: +46-31-823758
E-mail address: nyholm@medkem.gu.se (P.-G. Nyholm).

0008-6215/02/$ - see front matter
PII: S0008-6215(02)00089-7

2. Methods

The structural formula of the pentasaccharide repeating unit of the *S. dysenteriae* type 2 O-antigen is shown in Fig. 1. The conformational search was performed without the O-acetyl group, since the position of this group on the GlcNAc branch has not been unambiguously located. The notation used for the torsion angles of the glycosidic linkages is $\phi = $ H-1–C-1–O-1–C-*X*, $\psi = $ C-1–O-1–C-*X*–H-*X* with $X = 3$ and 4 in the $(1 \rightarrow 3)$- and $(1 \rightarrow 4)$-glycosidic linkages, respectively.

Initial calculations were carried out using the GLYCAN program.[4] However, the results indicated that this rigid residue approach is not suitable in the case of a highly constrained structure such as the type 2 O-antigen. To allow full relaxation of the residues, MM3 was chosen as the main method for this study. MM3[10–12] is considered to be one of the very best force fields for oligosaccharides.[13] MM3(96) was used to calculate the relaxed potential ϕ/ψ energy maps of all the constituent disaccharide moieties and for four-dimensional systematic search in the ϕ/ψ space of the trisaccharide moiety forming the branch. All the systematic searches were performed with a step size of 15°.

The disaccharides were calculated with driver option 4, which ensures that the starting conformation at each ϕ/ψ point is recalculated with correct geometry for the pyranose rings and the pendant groups. Different combinations of starting conformations for the primary and secondary hydroxyl groups were considered as described by French et al.,[14] and the lowest energy value obtained at each ϕ/ψ point was used in the generation of adiabatic potential energy ϕ/ψ maps.

In the case of the four-dimensional systematic search on the trisaccharides, the input was generated with in-house developed software selecting ϕ/ψ points within a range of 12 kcal/mol from the global minimum of the adiabatic energy map of the corresponding disaccharide units. For the trisaccharide, this permutation resulted in 40,182 starting conformations. The MM3 calculation were performed with input files defining multiple single-point minimizations with constrained geometry for the relevant ϕ/ψ glycosidic torsions. In calculations on the trisaccharide, the eight different combinations of the two favored rotamers for each primary hydroxyl group were considered. The orientation of the secondary hydroxyl groups was set as R (counter-clockwise),[14] since in our experience, the geometry of these groups has very little influence on the ϕ/ψ maps in the case of calculations at a dielectric constant of 80. Thus, the total number of starting conformations for the trisaccharide was 321,456. The glycosidic linkage downstream to the branching trisaccharide was studied with two-dimensional ϕ/ψ MM3 calculations on the tetrasaccharide which included the branch. These calculations considered the global minimum-energy conformation of the trisaccharide branch and additionally seven minor local-minimum conformations found for this structure in the systematic search.

MM3 energy minimization was performed on the hexasaccharide consisting of the repeating unit and one additional downstream residue (α-D-GalNAc) using as starting geometry the ϕ/ψ torsions of the global energy minima obtained in the systematic search. The geometry obtained for this hexasaccharide was used to build a sequence of eight consecutive repeating units.

In order to investigate possible alternative conformations for a longer sequence, the flexible linkages (i.e., the α-D-Glc-$(1 \rightarrow 4)$-β-D-Gal and the β-D-Gal-$(1 \rightarrow 3)$-α-D-GalNAc linkages; see Section 3) in a structure of six repeating units were randomly assigned one of three different ϕ/ψ values, which had been selected evenly distributed within the 1 kcal/mol range from the global minimum of the respective disaccharide adiabatic map. This procedure generated three[11] starting conformations of which 10,000 were randomly selected for full, unconstrained MM3 energy minimization. The resulting conformations within 1.5 kcal/mol from the lowest energy conformation were visually inspected.

All the MM3 calculations were performed with a dielectric constant ε of 80 to simulate an aqueous medium. The calculations were carried out on five computers with dual Intel 467–800 MHz processors using the LINUX version of MM3(96) (Allinger, Univ. of Georgia). The CPU time required for the ϕ/ψ systematic search for each C-5–C-6 rotamer of the trisaccharide was about 300 h. The template input files for MM3 were generated with the SYBYL software (Tripos Inc., St. Louis), which was also used for production of molecular graphics. The adiabatic energy surfaces were calculated with in-house developed software and the maps were generated with the program GSHARP (AVS Inc, Waltham, US).

After the modeling of the non-O-acetylated type 2 O-antigen, an O-acetyl group was attached on the α-D-GlcNAc residue either at C-3 or C-4. The favored conformations according to MM3 for the O-acetyl group in these positions were studied with respect to possible contacts with the saccharide main-chain by inspection with SYBYL.

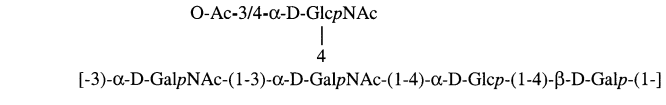

Fig. 1. Structural formula of the repeating unit of the *S. dysenteriae* type 2 O-antigen.[7] The O-acetyl group indicated alternatively at C-3 and C-4 of the α-D-GlcNAc branch has not been unambiguously located.

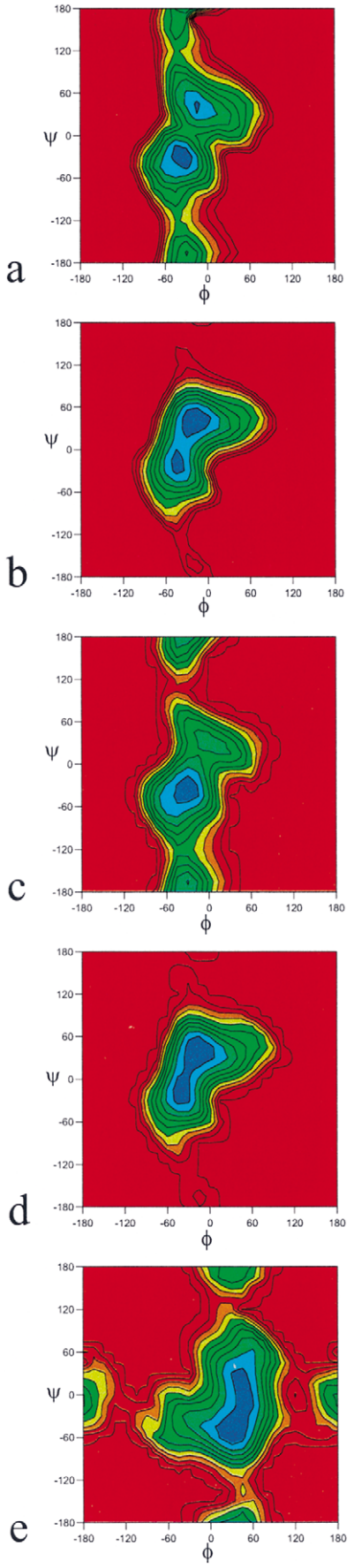

3. Results

Calculations with MM3 were carried out on all the disaccharide combinations occurring in the O-antigen. The obtained MM3 adiabatic energy ϕ/ψ maps are shown in Fig. 2(a–e). The map for the α-D-GalNAc-(1→3)-α-D-GalNAc linkage (Fig. 2(a)) shows its global minimum at $\phi/\psi \approx -30°/-30°$ and a secondary minimum at $\phi/\psi \approx -15°/30°$. The barrier between these minima is due to the proximity of the N-acetyl group of the downstream GalNAc to the hydroxymethylene group of the upstream GalNAc residue. The α-D-GlcNAc-(1→4)-α-D-GalNAc branch linkage (Fig. 2(b)) shows a global minimum at $\phi/\psi \approx -15°/45°$ separated by a low barrier from a secondary minimum at $\phi/\psi \approx -45°/-15°$. The α-D-GalNAc-(1→4)-α-D-Glc disaccharide (Fig. 2(c)) is rather restricted to a global minimum at $\phi/\psi \approx -30°/-30°$. The α-D-Glc-(1→4)-β-D-Gal and β-D-Gal-(1→3)-α-D-GalNAc linkages (Fig. 2(d and e)) have single elongated minimum energy wells and appear to be rather flexible with respect to the ψ torsion.

Systematic searches with MM3 on the trisaccharide at the branching point α-D-GalNAc-(1→3)-[α-D-GlcNAc-(1→4)-]-α-D-GalNAc yielded the adiabatic maps shown in Fig. 3. It can be noted that the ϕ/ψ-space of α-D-GalNAc-(1→3)-α-D-GalNAc in the trisaccharide (Fig. 3(a)) differs from that of the disaccharide (Fig. 2(a)) in having a disfavored secondary minimum ($\phi/\psi = 0°/15°$). Thus, this linkage has only one distinctly favored energy-well. Also, the α-D-GlcNAc-(1→4)-α-D-GalNAc linkage in the trisaccharide (Fig. 3(b)) shows essentially only one favored conformer at $\phi/\psi \approx -30°/45°$ in agreement with the global minimum found for the disaccharide (Fig. 2(b)). The secondary energy minimum calculated for this linkage at $\phi/\psi \approx -45°/-15°$ is significantly disfavored in the trisaccharide due to interference with the adjacent α-D-GalNAc-(1→3)-residue. MM3 calculations on the α-D-GalNAc-(1→4)-α-D-Glc linkage performed on the tetrasaccharide at the branching point (Fig. 3(c)) shows that this linkage has a ϕ/ψ energy surface practically identical to that of the corresponding isolated disaccharide (Fig. 2(c)).

The preferred ϕ/ψ angles found in the systematic search (Figs. 3(a–c) and 2(d–e)) were used as input for a final full MM3 minimization on a hexasaccharide comprising the repeating unit and one adjacent down-

Fig. 2. Adiabatic potential energy ϕ/ψ maps obtained with MM3 for the glycosidic linkages of the disaccharide moieties contained in the type 2 O-antigen. (a) α-D-GalNAc-(1→3)-α-D-GalNAc; (b) α-D-GlcNAc-(1→4)-α-D-GalNAc; (c) α-D-GalNAc-(1→4)-α-D-Glc; (d) α-D-Glc-(1→4)-β-D-Gal; and (e) β-D-Gal-(1→3)-α-D-GalNAc. Contour levels are shown at every kcal/mol with blue for low-energy regions and red for high-energy regions.

stream residue. The obtained final conformation is shown in Fig. 4 and the torsion angles are listed in Table 1. The results show that in each repeating unit the α-D-Glc-(1→4)-β-D-Gal moiety forms a bend of approximately 90° in the main-chain. The α-D-GlcNAc-(1→4) branch protrudes at the convex side of this bent structure.

Modeling of an O-acetyl group at C-3 and C-4 of the GlcNAc residue indicated that the O-acetyl group does not interfere with the main-chain of the saccharide in either of these positions. We therefore consider our calculations of the favored conformation of the O-unacetylated compound to be valid also for the natural O-acetylated type 2 O-antigen.

A model of eight repeating units was generated with SYBYL on the basis of the minimum energy conformation of the hexasaccharide containing the repeating unit and one downstream residue (Table 1). The obtained structure is a compact helix with a surprising threefold symmetry. Further MM3 energy minimization did not significantly change the geometries of the glycosidic linkages in this helical structure (Fig. 5). The helix is left-handed, has a pitch of 14 Å and a diameter of approximately 22 Å. In each turn of the helix, the three GlcNAc branches make van der Waals contacts with the adjacent upstream turn of the helix. Analysis of surface lipophilicity, shown as a color-coded solvent accessible surface (Fig. 5(c)), indicates that the branch point has a significant hydrophobic patch. This is mainly due to the N-acetyl groups of the GlcNAc branch and the upstream GalNAc residue. As shown in a side view, the exterior of the helix is hydrophilic with solvent-accessible pores, which extend towards the core of the helix.

In order to investigate alternative conformations for a sequence of repeating units, a random search was carried out with respect to the α-D-Glc-(1→4)-β-D-Gal and the β-D-Gal-(1→3)-α-D-GalNAc linkages, which have a considerable flexibility according to the adiabatic energy maps of the disaccharides (Fig. 2(d–e)). Inspection of the 50 obtained minimum-energy conformations at < 1.5 kcal/mol from the lowest energy conformation showed that all of these conformations contained a helical portion, but in most cases, the terminal regions were somewhat uncoiled. With one exception these helical structures (Fig. 6(a–b)) were similar to the regular helix with threefold symmetry obtained by multiplication of the repeating unit. The exception was the conformation with the lowest energy, favored by 0.6 kcal/mol, which showed a more irregular helical shape with 4 repeating units per turn (Fig. 6(c)). This conformation also shows hydrophobic patches at the branch points, but these surfaces are located more superficially than in the helix with three repeating units per turn.

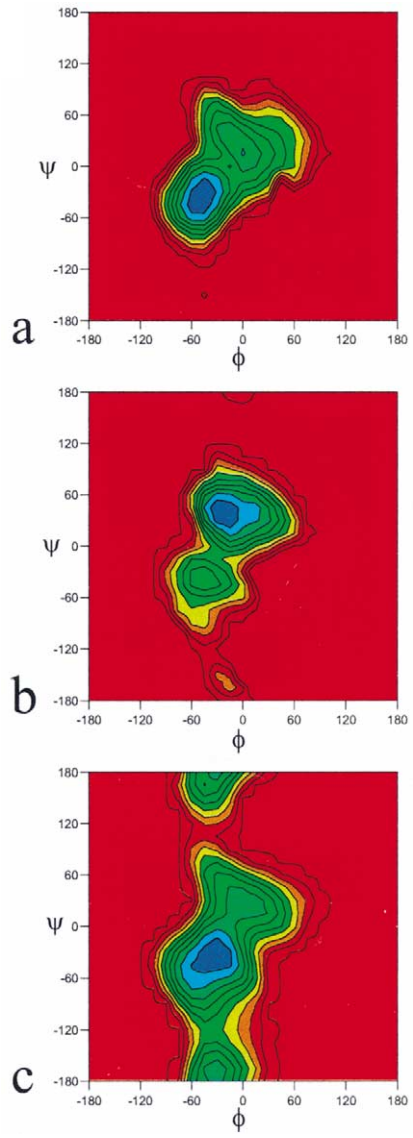

Fig. 3. Adiabatic potential energy ϕ/ψ maps obtained with MM3 for the glycosidic linkages of the trisaccharide α-D-GalNAc-(1→3)-[α-D-GlcNAc-(1→4)-]-α-D-GalNAc at the branching point of the type 2 O-antigen: (a) α-D-GalNAc-(1→3)-α-D-GalNAc. One major energy minimum is observed at $\phi/\psi \approx -30°/-30°$. (b) α-D-GlcNAc-(1→4)-α-D-GalNAc. The major minimum is at $\phi/\psi \approx -30°/45°$. The relative energy level of the second energy minimum ($\phi/\psi \approx -45°/-15°$) has increased significantly compared to the disaccharide (Fig. 2(b)). (c) shows the adiabatic ϕ/ψ energy map of the α-D-GalNAc-(1→4)-α-D-Glc linkage in the tetrasaccharide at the branching point. The map shows one major energy well which is practically identical to that of the corresponding disaccharide (Fig. 2(c)). Contour levels as in Fig. 2.

4. Discussion

The MM3 calculations on the tetrasaccharide at the branching point of the repeating unit of the type 2 O-antigen indicate that this moiety is highly constrained with essentially only one favored conformation (Figs. 3 and 4). With respect to the α-D-GalNAc-(1→

3)-α-D-GalNAc linkage, the calculated favored conformation is in good agreement with experimental results from X-ray and NMR studies on the structurally related α-D-GalNAc-(1→3)-β-D-GalNAc moiety of the terminal segment of the Forssman pentasaccharide.[15–17] The significant restrictions of the adiabatic energy maps of the α-D-GalNAc-(1→3)-α-D-GalNAc linkage in the type 2 O-antigen are partly due to the collision of the hydroxymethylene group of the GalNAc with the N-acetyl group of the downstream GalNAc residue (Fig. 2(a)). A similar interference has been observed in calculations on the α-D-Gal-(1→3)-α-D-GlcNAc linkage of the non-branched *S. dysenteriae* type 1 O-antigen.[4] Furthermore, the α-D-GalNAc-(1→3)-α-D-GalNAc linkage in the type 2 O-antigen is restricted due to interactions with the α-D-GlcNAc branch. Similarly, the α-D-GlcNAc-(1→4)-α-D-GalNAc branch linkage experiences significant restrictions in the trisaccharide

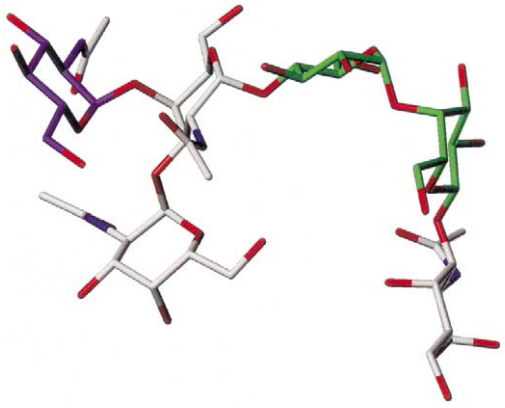

Fig. 4. MM3 minimum energy conformation of a hexasaccharide, including the repeating unit of the type 2 O-antigen and an additional downstream α-D-GalNAc residue. For torsion angles see Table 1. The α-D-Glc-(1→4)-α-D-Gal moiety (green) forms a 90° bend of the main chain. It should be noted that in the isolated hexasaccharide the two glycosidic linkages α-D-Glc-(1→4)-β-D-Gal and β-D-Gal-(1→3)-α-D-GalNAc, which are not involved in the branch points, are expected to show a significant flexibility according to the φ/ψ energy maps (Fig. 2(d and e)). The branch residue (α-D-GlcNAc) is shown in purple. Hydrogen atoms have been omitted.

Table 1
φ/ψ torsion angles of the glycosidic linkages in the MM3 minimum energy conformation of the hexasaccharide which includes the repeating unit and one downstream residue of the type 2 O-antigen

Linkage	φ (°)/ψ (°)
α-D-GalNAc-(1→3)-α-D-GalNAc	−44/−29
α-D-GlcNAc-(1→4)-α-D-GalNAc	−25/38
α-D-GalNAc-(1→4)-α-D-Glc	−31/−33
α-D-Glc-(1→4)-β-D-Gal	−15/42
β-D-Gal-(1→3)-α-D-GalNAc	32/−47

(Figs. 2(b) and 3(b)). In the case of the α-D-GalNAc-(1→4)-α-D-Glc linkage, the calculations indicate that the preferred φ/ψ conformation is not affected significantly by the branch. The present calculations were performed at a dielectric constant of 80, which essentially disregards the contribution from intramolecular hydrogen bonds. However, the depth of the energy wells suggests that it is very unlikely that these calculated conformational preferences would be significantly changed by intramolecular hydrogen bonding, which is considered to be weak for saccharides in an aqueous environment.[18]

Within a sequence of repeating units the α-D-Glc-(1→4)-β-D-Gal linkages and the adjacent β-D-Gal-(1→3)-α-D-GalNAc linkages are conformationally more flexible (Fig. 2(d, e)) than the glycosidic linkages around the branch points (Fig. 3). This flexibility could theoretically result in a multitude of conformations. However, the conformational analysis of a sequence of six repeating units showed that most of the calculated low-energy conformations were very similar to the regular helix with threefold symmetry generated from the minimum-energy geometry of the repeating unit (Table 1, Fig. 5). This helical type of structure appears to be stabilized by a hydrophobic effect arising from the lipophilic surfaces at the branch points (Fig. 5(c)) which are in close contacts with the adjacent upstream turn of the helix. Although these opposing surfaces are not particularly hydrophobic, they are obviously less polar than bulk water which should give rise to a favorable hydrophobic effect and possibly a low-polarity interface favoring significant hydrogen bonding. It should also be noted that the complete type 2 O-antigen contains an additional O-acetyl group at C-3 or C-4 on the GlcNAc branch, which should contribute to the hydrophobic stabilization, especially if the substitution is at C-3. Hydrophobic effects are not accounted for in MM3 calculations, but such interactions can be expected to result in an additional stabilization of the helix considering the fact that the hydrophobic effect amounts to 0.8 kcal/mol per CH_2 group.[19] The second type of favored helical structure (Fig. 6(c)), which is more irregular and has 4 repeating units/turn, appears to have weaker intramolecular hydrophobic interactions. In solution, it is possible that the helical structures are interrupted by kinks arising dynamically in the chain due to flexibility of the hinge regions. Further studies with computations and NMR will be needed to investigate the stability of the described helical structures with special attention to the role of intramolecular hydrophobic interactions.

No doubt the helical structures found in the modeling may have functional implications with respect to the immunological properties of this O-antigen. The α-D-Glc-(1→4)-β-D-Gal moiety, which is exposed at the convex side of the type 2 repeating unit (Fig. 4) and

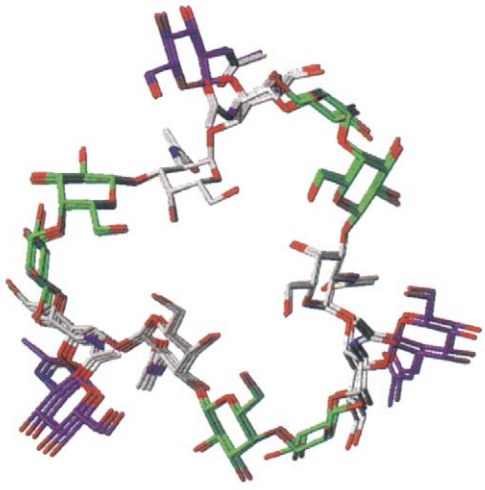

(a)

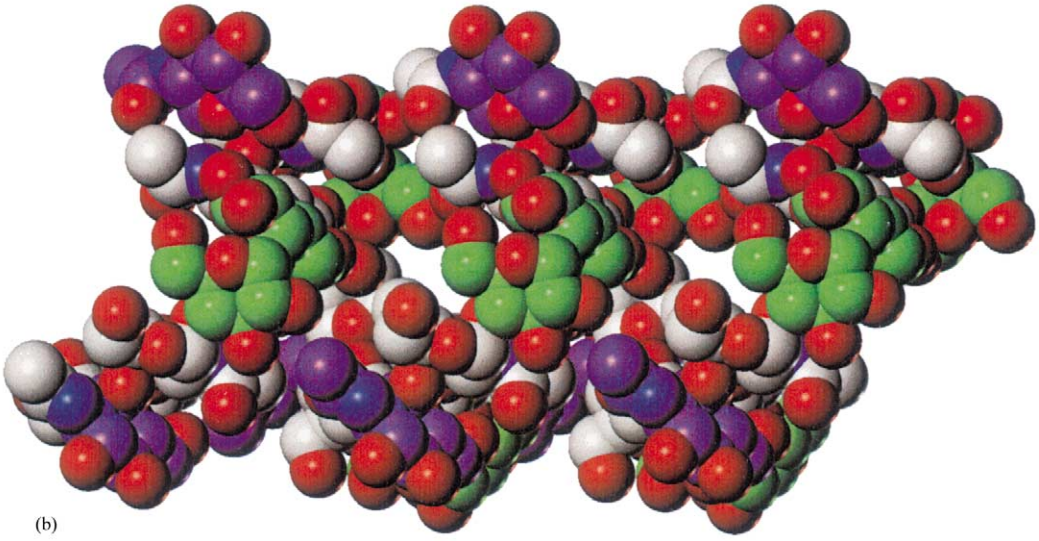

(b)

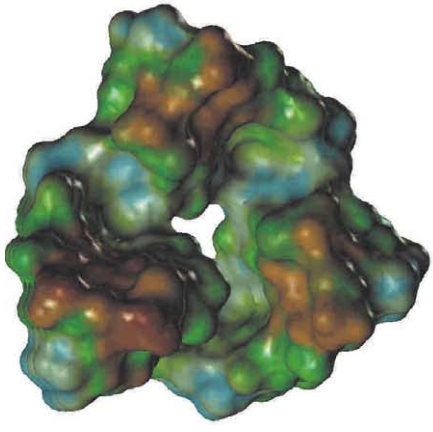

(c)

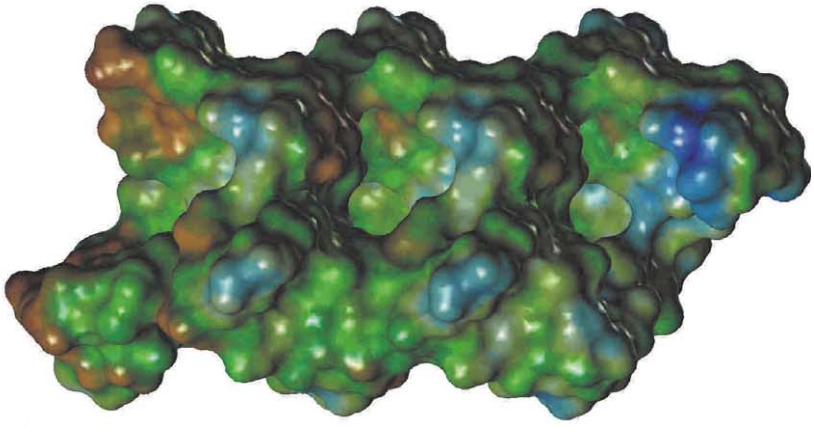

(d)

Fig. 5.

on the surface of the predicted helices (Figs. 5 and 6), is structurally similar to galabiose (α-D-Gal-(1→4)-β-D-Gal), which occurs in mammalian globo-glycolipids[20] and glycoproteins.[21] The only structural difference is the configuration at C-4 of the upstream residue with places the O-4 in an axial orientation in the case of galabiose. From NMR[15,16] and X-ray studies[22,23] galabiose is known to have a favored conformation resulting in a 90° bend in agreement with the presently calculated favored ϕ/ψ conformation for the α-D-Glc-(1→4)-β-D-Gal moiety. It thus appears that the α-D-Glc-(1→4)-β-D-Gal moiety of the type 2 O-antigen is isosteric with galabiose except for the Glc O-4 (Fig. 7). In several studies it has been shown that the galabiose moiety occurs in complex saccharides of bacterial origin, e.g., in the lipo-oligosaccharides of *Hemophilus influenzae* and in *Neisseria*.[24–26] On the basis of these studies, it has been suggested that this saccharide moiety allows the bacteria to evade the immune responses of the host due to the fact that this moiety is a "mimotope", which mimics an endogenous epitope.[27] In the case of the *S. dysenteriae* type 2 O-antigen, the α-D-Glc-(1→4)-β-D-Gal moiety might play a similar role by mimicry of galabiose (cf. Figs. 4 and 7). In a similar way the α-D-GalNAc-(1→3)-α-D-GalNAc moiety of the type 2 O-antigen is essentially isosteric with the terminal α-D-GalNAc-(1→3)-β-D-GalNAc segment of the Forssman antigen of the host (Fig. 7). This potential mimotope in the type 2 O-antigen might be significant for the terminal repeating unit, whereas for internal repeating units this epitope appears to become cryptic due to helical stacking (Fig. 5). Further studies will be required to determine the immunological properties of the potential mimotopes of the type 2 O-antigen.

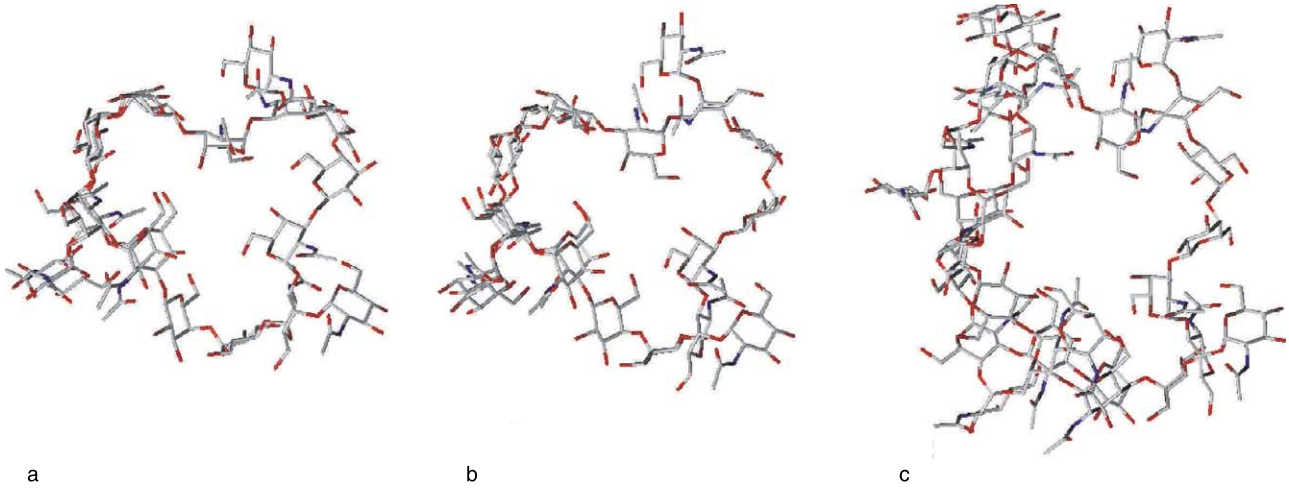

Fig. 6. Different helical conformations obtained through conformational analyses of a sequence of six repeating units: (a–b) Two helical conformations with four repeating units which are very similar to the regular threefold symmetric helix described in Fig. 5, although individual glycosidic torsion angles differ significantly. Two repeating units at the termini of the sequence had a somewhat uncoiled conformation and were excluded from display for clarity. The MM3 conformational energies of the helices shown are somewhat higher (< 1.5 kcal/mol) than for a corresponding fragment of the regular threefold symmetric helix shown in Fig. 5. (c) A second type of helical conformation calculated for a sequence of six repeating units. This conformation, which has slightly lower MM3 energy (0.6 kcal/mol) than the threefold symmetric helix, is fairly irregular and contains 4 repeating units/turn. It can be noted that the GlcNAc branches are more superficially located and probably they do not contribute to stabilization of the helix by hydrophobic interactions as much as in the case of the helix with 3 repeating units/turn.

Fig. 5. Modeled conformation of eight consecutive repeating units of the type 2 O-antigen forming a compact helical structure: (a) axial view in stick display and (b) side view in space filling model obtained by 90° clockwise rotation of (a) about the *y*-axis. The left-handed helix contains 3.0 repeating units per turn and has a pitch of 14 Å and a diameter of about 22 Å. MM3 minimization indicated that this helix represents a stable minimum-energy conformation. Note that the α-D-Glc-(1→4)-β-D-Gal moieties (green) and the α-D-GlcNAc branches (purple) are exposed on the outside of the helix, while the α-D-GalNAc-(1→3)-α-D-GalNAc moieties of the main chain are buried internally in the helix. (c) An axial view of the solvent accessible surface calculated with MOLCAD (Tripos, Inc.). The surface contains three lipophilic patches (brown) formed by the GlcNAc branches while the rest of the surface is more hydrophilic (green). (d) A side view of the helix with solvent accessible surface. The lateral surfaces of the helix have an intermediate or high hydrophilicity (green and blue, respectively). The GlcNAc branches form "bridges" of non-covalent contacts between adjacent turns of the helix. In between these bridges are the orifices of deep crypts of aqueous space which extend into the core of the helix.

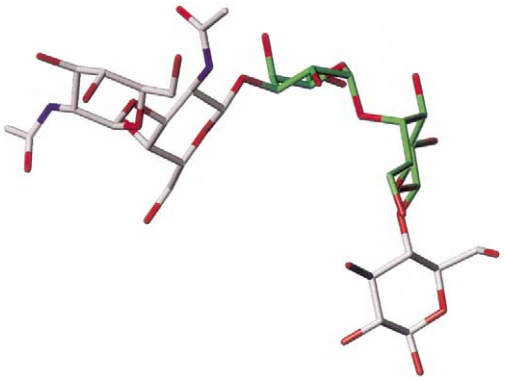

Fig. 7. mm3 minimum energy conformation of the Forssman oligosaccharide with the galabiose moiety indicated with green carbons. The galabiose moiety and the α-D-Glc-(1→4)-β-D-Gal moiety of the type 2 O-antigen (cf. Fig. 4) are essentially isosteric (except for the configuration of the Glc O-4) suggesting a mimicry which might allow the type 2 O-antigen to evade the immune response of the host. Furthermore, the α-D-GalNAc-(1→3)-α-D-GalNAc portion of the type 2 O-antigen is essentially isosteric with the terminal segment α-D-GalNAc-(1→3)-β-D-GalNAc of the Forssman saccharide (grey). Also this portion might serve as a mimotope in the type 2 O-antigen. However, since this disaccharide is turned towards the interior of the helical structure of the type 2 O-antigen this epitope appears inaccessible on internal repeating units.

Acknowledgements

This work is supported by a grant from the Swedish Medical Research Council (006). We are indebted to Professor I. Pascher for valuable comments on the manuscript.

References

1. Kotloff K. L.; Winickoff J. P.; Ivanoff B.; Clemens J. D.; Swerdlow D. L.; Sansonetti P. J.; Adak G. K.; Levine M. M. *Bull. WHO* **1999**, *77*, 651–666.
2. Pozsgay V.; Chu C.; Pannell L.; Wolfe J.; Robbins J. B.; Schneerson R. *Proc. Natl. Acad. Sci.* **1999**, *96*, 5194–5197.
3. Coxon B.; Sari N.; Batta G.; Pozsgay V. *Carbohydr. Res.* **2000**, *324*, 53–65.
4. Nyholm P. G.; Mulard L. A.; Miller C. E.; Lew T.; Olin R.; Glaudemans C. P. J. *Glycobiology* **2001**, *11*, 945–955.
5. Pavliak V.; Nashed E. M.; Pozsgay V.; Kovac P.; Karpas A.; Chu C.; Schneerson R.; Robins J. B.; Glaudemans C. P. *J. Biol. Chem.* **1993**, *268*, 25797–25802.
6. Miller C. E.; Mulard L. A.; Padlan E. A.; Glaudemans C. P. *Carbohydr. Res.* **1998**, *309*, 219–226.
7. Dmitriev B. A.; Knirel Y. A.; Kochetkov N. K.; Hofman I. L.; Capek K. *Eur. J. Biochem.* **1977**, *76*, 433–440.
8. Knirel Y. A.; Kochetkov N. K. *Biochemistry (Moscow)* **1994**, *59*, 1325–1383.
9. Paulsen H.; Buensch H. *Chem. Ber.* **1981**, *114*, 3126–3145.
10. Allinger N. L.; Yuh Y. H.; Lii J. H. *J. Am. Chem. Soc.* **1989**, *111*, 8551–8566.
11. Allinger N. L.; Rahman M.; Lii J. H. *J. Am. Chem. Soc.* **1990**, *112*, 8293–8307.
12. Lii J. H.; Allinger N. L. *J. Comput. Chem.* **1991**, *12*, 186–199.
13. Perez S.; Imberty A.; Engelsen S. B.; Gruza J.; Mazeau K.; Jimenez-Barbero J.; Poveda A.; Espinosa J. F.; van Eyck B. P.; Johnson G.; French A. D.; Louise M.; Kouwijzer C. E.; Grootenuis P. D. J.; Bernardi A.; Raimondi L.; Senderowitz H.; Durier V.; Vergoten G.; Rasmussen K. *Carbohydr. Res.* **1998**, *314*, 141–155.
14. French, A. D.; Tran, V. H.; Perez, S. In *Computer Modelling of Carbohydrate Molecules*; ACS Symposium Series 430; American Chemical Society: Washington, DC, 1990; pp 191–212.
15. Poppe, L.; Dabrowski, J.; von der Lieth, C. W. *Biochem. Biophys. Res. Commun.* **1991**, *174*, 1169–1175.
16. Grönberg G.; Nilsson U.; Bock K.; Magnusson G. *Carbohydr. Res.* **1994**, *257*, 35–54.
17. Hamelryck T. W.; Loris R.; Bouckeart J.; Dao-Thi M. H.; Strecker G.; Imberty A.; Fernandez E.; Wyns L.; Etzler M. *J. Mol. Biol.* **1999**, *286*, 1161–1177.
18. Kirschner K.; Woods R. J. *Proc. Natl. Acad. Sci.* **2001**, *98*, 10541–10545.
19. Tanford C. *The Hydrophobic effect*, 2nd ed.; Wiley: New York, 1980.
20. Hakomori S. *Glycoconjugate J.* **2000**, *17*, 627–647.
21. Takahashi N.; Khoo K. H.; Suzuki N.; Johnson J. R.; Lee Y. C. *J. Biol. Chem.* **2001**, *276*, 23230–23239.
22. Svensson G.; Albertsson J.; Svensson C.; Magnusson G.; Dahmen J. *Carbohydr. Res.* **1986**, *146*, 29–38.
23. Dodson K.; Pinker J. S.; Rose T.; Magnusson G.; Hultgren S.; Waksman G. *Cell* **2001**, *105*, 733–743.
24. Mandrell R. E.; Griffiss J. M.; Macher B. A. *J. Exp. Med.* **1988**, *168*, 107–126.
25. Virji M.; Weiser J. N.; Lindberg A. A. *Microb. Pathogen.* **1990**, *9*, 441–450.
26. Masoud H.; Moxon E. R.; Martin A.; Krajcarski D.; Richards J. C. *Biochemistry* **1997**, *36*, 2091–2103.
27. Rahman M.; Jonsson A. B.; Holme T. *Microb. Pathogen.* **1998**, *24*, 299–308.